http://eprints.gla.ac.uk/80463/

Deposited on: 7 May 2014

GENE DELIVERY

ELSEVIER

CrossMark

Identification of novel small molecule inhibitors of adenovirus gene transfer using a high throughput screening approach ☆

Margaret R. Duffy [a], Alan L. Parker [a,b], Eric R. Kalkman [c], Katie White [a], Dmytro Kovalskyy [d,1], Sharon M. Kelly [e], Andrew H. Baker [a,*]

[a] British Heart Foundation Glasgow Cardiovascular Research Centre, Institute of Cardiovascular and Medical Sciences, University of Glasgow, 126 University Place, Glasgow G12 8TA, UK
[b] Institute of Cancer & Genetics, Tenovus Building, Heath Park, Cardiff CF14 4XN, UK
[c] Wellcome Trust Centre for Molecular Parasitology, Institute of Infection, Immunity & Inflammation, College of Veterinary and Life Sciences, University of Glasgow, 120 University Place, Glasgow G12 8TA, UK
[d] ChemBio Centre, National Taras Shevchenko University, Chervonotkatska 61, Kiev 02090, Ukraine
[e] Institute of Molecular, Cell and Systems Biology, College of Medical, Veterinary and Life Sciences, University of Glasgow, Glasgow G12 8QQ, UK

ARTICLE INFO

ABSTRACT

Due to many favourable attributes adenoviruses (Ads) are the most extensively used vectors for clinical gene therapy applications. However, following intravascular administration, the safety and efficacy of Ad vectors are hampered by the strong hepatic tropism and induction of a potent immune response. Such effects are determined by a range of complex interactions including those with neutralising antibodies, blood cells and factors, as well as binding to native cellular receptors (coxsackie adenovirus receptor (CAR), integrins). Once in the bloodstream, coagulation factor X (FX) has a pivotal role in determining Ad liver transduction and viral immune recognition. Due to difficulties in generating a vector devoid of multiple receptor binding motifs, we hypothesised that a small molecule inhibitor would be of value. Here, a pharmacological approach was implemented to block adenovirus transduction pathways. We developed a high throughput screening (HTS) platform to identify small molecule inhibitors of FX-mediated Ad5 gene transfer. Using an in vitro fluorescence and cell-based HTS, we evaluated 10,240 small molecules. Following sequential rounds of screening, three compounds, T5424837, T5550585 and T5660138 were identified that ablated FX-mediated Ad5 transduction with low micromolar potency. The candidate molecules possessed common structural features and formed part of the one pharmacophore model. Focused, mini-libraries were generated with structurally related molecules and in vitro screening revealed novel hits with similar or improved efficacy. The compounds did not interfere with Ad5:FX engagement but acted at a subsequent step by blocking efficient intracellular transport of the virus. In vivo, T5660138 and its closely related analogue T5660136 significantly reduced Ad5 liver transgene expression at 48 h post-intravenous administration of a high viral dose $(1 \times 10^{11}$ vp/mouse). Therefore, this study identifies novel and potent small molecule inhibitors of the Ad5 transduction which may have applications in the Ad gene therapy setting.

© 2013 The Authors. Published by Elsevier B.V. All rights reserved.

1. Introduction

Adenoviruses have been developed, engineered and partially optimised for use as gene therapy vectors, viral oncolytics and vaccines. Several features make them attractive tools for such a broad range of applications including the relative ease of genetic manipulation, large packaging capacity, transduction efficiency and high level transgene expression. Furthermore, Ads can be produced at high titres under Good Manufacturing Practice conditions, an attribute key for successful development in the biotechnology industry and for clinical translation. As a result they are currently the most widely used vector in clinical gene therapy protocols, with the majority of studies based on Ad serotype 5 [1]. Nevertheless, despite the many favorable characteristics and promising results of preclinical trials, efficacy in the clinic has been variable indicating that the full translational potential of these viruses is yet to be reached.

There are several pitfalls which need to be overcome in order to improve the viability of Ad5 as a therapeutic gene delivery vector [2]. For many gene therapy targets such as disseminated cancers the optimal route for targeting the multitude of micro-metastases is intravascular delivery. However, the safety and efficacy of Ad5 following intravascular administration are hampered by two major factors,

these being the substantial propensity of the virus to transduce the liver, along with immune recognition of the virus [3–6]. A series of complex host "off target" interactions define this inherent hepatic tropism and immunogenicity. Pre-existing neutralising antibodies and the resident liver macrophages, Kupffer cells, sequester a large proportion of the viral load and contribute to the host inflammatory response [5]. Virus binding to blood components such as erythrocytes [7,8], platelets [9,10], complement [11] and coagulation factors [12,13] all impact strongly on the ability of the virus to circulate. In recent years, several studies have focused on the role of factor X (FX), a central component of the coagulatory system, in determining the Ad tropism [14]. Upon contact with the blood Ad5 transduction of the liver is mediated by a direct high affinity interaction between the virus and FX [13]. The FX γ-carboxylated glutamic acid domain binds to the hexon protein and the FX serine protease domain tethers the Ad5:FX complex to heparan sulphate proteoglycans (HSPGs) on the surface of hepatocytes, resulting in subsequent cell binding and receptor-mediated virus internalisation [12–16]. Crystallographic and cryoelectron microscopy techniques have been employed to identify the key amino acid residues within the hexon responsible for binding FX [17,18]. Generation of Ad5 vectors devoid of FX-binding effectively ablated liver transduction *in vivo* [17,19]. Interestingly, recent work has also implicated an important role for FX in the induction of viral innate immune and inflammatory responses [18]. Genome wide transcriptional profile analysis *in vivo* revealed significant differences in the genes activated by Ad5 and a FX-binding ablated Ad5 vector [18]. In contrast to the parental vector, the non-FX binding Ad5 failed to activate NFκB-dependant early response genes encoding several Ad associated inflammatory cytokines and chemokines [18]. This may be related to the newly identified role for FX in the protection of Ad5 from attack by natural antibodies and complement [6]. In contrast to studies in wild-type mice, FX coating of the virus was not found to be essential for liver transduction in mice deficient in antibodies, C1q and C4 [6].

It is therefore evident that a series of differential and sophisticated host mechanisms exist which have important roles in determining Ad tropism, immunogenicity and ultimately vector efficacy and safety *in vivo*. Ideally, a vector could be administered intravascularly and bypass its native tropism to selectively target the desired cells/tissues in the absence of an immune response. Due to the complexity in the development and generation of a vector devoid of multiple receptor binding sites, one alternate approach was to develop a small molecule inhibitor to block FX-mediated Ad5 transduction. Here we implemented a high throughput strategy to screen a pharmacologically diverse library of "drug-like" compounds in search of a compound capable of manipulating the FX-mediated Ad5 transduction pathway.

2. Materials

Purified human blood coagulation FX was purchased from Cambridge Biosciences (Cambridge, UK). The Pharmacological Diversity Drug-like Set was purchased from Enamine (Kiev, Ukraine). Hoechst 33342 and propidium iodide were obtained from Sigma Aldrich (Poole, UK).

3. Methods

3.1. Ethics statement

All animal experiments were approved by the University of Glasgow Animal Procedures and Ethics Committee and performed in strict accordance with UK Home Office guidelines.

3.2. Cell lines, cell culture and virus production

A549 (human lung carcinoma ATCC CCL-185) and SKOV3 (human ovarian carcinoma: ATCC HTB-77) cells were grown in RPMI 1640 medium supplemented with 10% foetal calf serum, 2 mM L-glutamine and 1% penicillin–streptomycin (Invitrogen, Paisley, UK). HEK293 (human embryonic kidney: ATCC CRL-1573) cells were grown in Dulbecco's Modified Eagle's Medium (DMEM; Invitrogen, Paisley, UK) supplemented with 10% foetal calf serum, 2 mM L-glutamine and 1% penicillin–streptomycin. High titre stocks of recombinant E1/E3-deleted Ad5 were produced by large-scale expansion of a plaque pure stock of Ad5 in HEK293 cells. Viruses were purified by CsCl gradient centrifugation. Viral particles (vp) were determined by microbicinchoninic-acid assay (Perbio Science, Cramlington, UK) using the formula 1 µg protein $= 4 \times 10^9$ vp [20]. End-point dilution assays were performed to quantify plaque-forming units (PFU)/ml. All preparations of Ad5 used in this study had similar vp:PFU titre ratios of approximately 50:1.

3.3. Compound library

The Pharmacological Diversity Drug-like Set (Enamine, Kiev) library consisted of 10,240 compounds preplated in columns 3 to 22 of 32 Matrix 384-well plates as single compounds at a concentration of 10 mM in 100% DMSO. Each plate had an individual barcode and sample ID for tracking purposes. Plates were sealed and compounds stored under nitrogen (BOC, Glasgow, UK) at −20 °C. All compounds were assured by the vendor (Enamine) to be at least 90% pure as assessed by liquid chromatography–mass spectrometry and proton nuclear magnetic resonance spectrometry. Analogue compounds of the hits from the screen were also purchased from Enamine. Briefly, the Pharmacological Diversity Drug-like Set was designed with the concept that active compounds against orphan targets may have topological properties similar to known small molecules (manuscript in preparation). That is, chemical space of known drugs can be used as a restriction factor upon selection of screening candidates for HTS campaigns against novel targets. To design the set, compounds from the Enamine stock collection (~1,000,000 compounds) were used. Using the program PASS (http://www.pharmaexpert.ru/passonline/reference.php) over 3000 biological activities for every compound in the stock were predicted [21]. As a result each compound has a "pharmacological profile" and any activity was denoted in binary mode as either *active* or *inactive*. Next, profile clustering was performed irrespective of the compounds' chemical structure. 10,240 centroids from this clusterisation were selected. Absorption, distribution, metabolism, and excretion (ADME) properties of compounds were predicted with QikProp (Schrodinger Inc.).

3.4. HTS assay

SKOV3 cells were seeded at a density of 1500 cells/well in 50 µl complete media in 384 µ-clear flat bottom black plates (Greiner bio-one, UK). Cells were tested prior to use to ensure that they were mycoplasma free. All robotics protocol design, scheduling and execution were performed using Biomek Software (Beckman Coulter, USA), SAMI Workstation EX Software (Beckman Coulter) and Biomek FXP Laboratory Automation Workstation (Beckman Coulter). Compound dilution plates (in serum free (SF) RPMI) were generated. Ad5GFP was added to columns 2 to 23 of the compound dilution plate. Cells in the assay plate were washed in SF media. 22.5 µl of SF media was added to each well of the control columns 1, 2, 23 and 24 and 22.5 µl of SF media containing FX was added to each well in columns 3 to 22. Columns 1 and 24 contained the untreated control samples. Columns 2 and 23 contained the test control samples. Into every second well of columns 2 and 23, 2.5 µl of SF media containing FX was added (final concentration of 10 µg/ml FX and 1% (v/v) DMSO vehicle) and into every other well of those columns, 2.5 µl of SF media was dispensed (−FX controls). 1000 vp/cell of Ad5 with/without compound was added to the cells. The virus used in this assay came from a single preparation of Ad5. Each compound was tested in triplicate, with each replicate on a separate plate. All wells in columns 3 to 22 had a concentration of 10 µM compound, 10 µg/ml FX and 1% (v/v) DMSO. Plates were incubated at 37 °C for 3 h. After

this incubation, 25 µl of complete media containing 20% (v/v) FCS, 1% (v/v) penicillin, 100 µg/ml streptomycin and 2 mM L-glutamine was added to all wells. Assay plates were further incubated at 37 °C. 48 h post-infection cells were fixed in 4% PFA for 15 min at room temperature. 10 µg/ml Hoechst 33342 and 10 µg/ml propidium iodide were added to the cells and incubated at room temperature for 20 min. Cells were washed in PBS before being imaged with the In Cell Analyser 2000 (GE Healthcare, Pittsburgh, USA). A single image of the central field of view in each well was captured using the 10× objective. Imaging conditions were as follows, filter sets were matched to each fluorophore; $350_{excitation\ (ex)}$ nm and $455_{emission\ (em)}$ nm for Hoechst 33342 nuclear staining, 490_{ex} nm and 525_{em} nm for GFP expression and 579_{ex} nm and 624_{em} nm for propidium iodide non-viable nuclear staining. To quantify the amount of GFP expression per viable cell, the images were analysed using IN Cell Developer Toolbox V1.6 software (GE Healthcare). This resulted in a numerical output enabling the calculation of results.

3.5. HTS data analysis

All test data were normalised to intraplate Ad5−FX, Ad5+FX and vehicle controls and expressed as percentage inhibition of FX-mediated Ad5GFP expression (% inhibition = (positive control − test compound) / (positive control − negative control)). To evaluate the robustness of the assay we calculated the Z′ factor in initial optimisation experiments [22]. The calculations were done according to the following formula: $Z' = 1 - ((3\delta pos + 3\delta neg) / (\mu pos - \mu neg))$, where δpos is the standard deviation for the Ad5+FX control, δneg is the standard deviation for the Ad5−FX control, µpos is the mean signal for the Ad5+FX control and µneg is the mean signal for the Ad5−FX control. The signal to background ratio (S:B = µpos/µneg) was also calculated. Any compounds causing greater than 75% inhibition of FX-mediated Ad5GFP expression were selected for second round screening analysis.

3.6. Analysis of Ad5 transduction in vitro

Cells were seeded in 96-well plates at a density of 2×10^4 cells/well and incubated overnight at 37 °C. Cells were washed with PBS and incubated with 1000 vp/cell Ad5lacz in SF medium in the absence or presence of 10 µg/ml FX with DMSO, T5550585, T5424837, T5660138, T5677956, T5660136 or T5572402 (Enamine) for 3 h at 37 °C. 100 µl of complete medium containing 20% serum was added to the cells and then incubated at 37 °C for a further 45 h. Cells were harvested by lysing in 100 µl 0.2% Triton-X-100. β-Galactosidase was quantified using Tropix Galacto-light Plus (Applied Biosystems, Warrington, UK) and a Wallac VICTOR2 plate reader (PerkinElmer Life and Analytical Sciences, Boston MA). β-Galactosidase activity was then normalised to total protein content of the samples, measured by bicinchoninic acid assay as per manufacturer's instructions, producing relative light units per milligram protein (RLU/mg protein). In some cases data were normalised to Ad5−FX and Ad5+FX controls and expressed as percentage inhibition of FX-mediated Ad5 expression. IC_{50} values were calculated by fitting a 4-parameter logistic non-linear regression model equation using MasterPlex ReaderFit analysis software.

3.7. MTT (3-(4,5-dimethylthiazol-2-yl)-2,5-diphenyltetrazolium bromide) assay

SKOV3 cells were plated at a seeding density of 2×10^4 in 96-well plates and incubated at 37 °C overnight. Cells were incubated with either DMSO or transduced with virus in the presence of 10 µM compound. After 48 h the medium on the cells was replaced with 100 µl complete medium and 15 µl of the MTT reagent. Cells were incubated for 4 h at 37 °C, after which 100 µl of Solubilization Solution/Stop Mix was added to each well and cells were incubated for a further 1 h at

37 °C. The cell viability was measured as colour intensity using a Wallac VICTOR² plate reader (Wallac) at a wavelength of 570 nm and which is directly proportional to the amount of live cells in the sample.

3.8. Surface plasmon resonance (SPR) analysis of Ad5:FX binding

SPR was performed using a Biacore 2000 (GE Healthcare, London, UK). Human FX was covalently immobilised on to the flowcell of a CM5 biosensor chip by amine coupling according to the manufacturer's instructions [12]. The immobilisation density was 500 response units. Sensorgrams were generated at a flow rate of 30 µl/min using 10 mM HEPES pH 7.4, 150 mM NaCl, 5 mM CaCl₂, and 0.05% Tween-20 as running buffer and regeneration between injections with HEPES pH 7.4, 150 mM NaCl, 3 mM EDTA, and 0.05% Tween-20. Injections of 10 µM compounds T5550585, T5424837, T5660138, T5677956, T5660136 or T5572402 (Enamine) or an equivalent volume of DMSO in the presence of Ad5 diluted in running buffer were passed over the chip. This was followed by regeneration of the biosensor chip. DMSO subtracted sensorgrams were generated and data analysed using Biacore 2000 Evaluation software.

3.9. Quantification of Ad5 colocalisation with the microtubule organising centre (MTOC)

Cells were seeded in 8-well chamber slides at 4×10^4 cells/well and incubated at 37 °C overnight. Cells were washed with PBS and incubated with 1×10^4 vp/cell of fluorescently-labelled Ad5 in 150 µl SF media for 1 h on ice in the absence or presence of 10 µg/ml FX with or without 10 µM pharmacological compound. Cells were incubated at 37 °C for 180 min prior to washing and fixation. Localisation of Ad particles at the MTOC was characterised by staining cells using a polyclonal rabbit pericentrin antibody (1:200 dilution: Abcam, Cambridge, UK) [16]. Cells were imaged using a Zeiss confocal microscope (LSM510). Colocalisation of Ad5 with the MTOC was quantified by visually assessing the percentage of cells with Alexa488-virus and pericentrin co-staining. Data were averaged from five microscope fields of view (40× objective) per experimental condition.

3.10. Circular dichroism analysis

Spectra were measured in quartz cells of 1 mm path length in a Jasco J-810 spectropolarimeter. Virus particles were measured using a concentration of 1×10^8 vp/sample in the presence of 10 µM T138, 10 µM T136 or an equivalent volume of DMSO in PBS. Samples were heated from 35 °C to 55 °C at increments of 2 °C using a Peltier device. Samples were allowed to equilibrate for 2 min at each temperature prior to measurement.

3.11. In vivo studies

Mice were injected via lateral tail vein injection with 1×10^{11} vp/mouse of Ad5 expressing a luciferase transgene in the absence or presence of 0.1% DMSO, 10 µM compound T5660138 or T5660136 in a final volume of 200 µl PBS or PBS alone. 48 h post-administration mice were injected subcutaneously with 300 µl of XenoLight D-Luciferin (Caliper, Life Sciences, Hopkinton, MA, USA). Mice were subject to whole body bioluminescence quantification (IVIS Spectrum, Caliper Life Sciences). Luciferin activity was measured using the IVIS Imaging System (IVIS Spectrum, Caliper) and expressed as average radiance (photons per second per centimetre squared per steradian ($p/s/cm2/sr$)). Blood samples were taken from mice at 48 h and serum separated from whole blood using a BD SST Microcontainer with clot activator (BD Diagnostics, Oxford, UK). Serum transaminases, aspartate aminotransferase (AST) and alanine aminotransferase (ALT), were quantified from 80 µl serum by the Veterinary Diagnostic Service

at the University of Glasgow. Animals were perfused to exsanguination with PBS and their livers and spleens used for immunohistochemistry on frozen tissue.

3.12. Luciferase immunofluorescence

Immunohistochemistry for luciferase expression was achieved by staining 4 μm liver or 6 μm spleen frozen sections with a mouse anti-luciferase (Luci17; Santa Cruz Biotechnology, Heidelberg, Germany) IgG$_1$, used at a final concentration of 1.33 μg/ml. Sections were fixed with ice-cold acetone at −20 °C for 10 min and allowed to air dry for 1 h. Endogenous avidin/biotin activity was blocked using a commercial kit (Vector Laboratories, Peterborough, UK). Staining was performed using the M.O.M Fluorescein Immunodetection kit (Vector Laboratories). Fluorescence was visualised using an Olympus BX60 fluorescence microscope (×40 magnification) and images acquired using Cell'M software (Olympus, London, UK). An isotype control antibody was used at identical final concentrations. Images were processed to reduce background using ImageJ and adjustments were applied equally to all compared images. Quantification of Alexa-488 positive regions was calculated as follows: at least 10 separate images (3 animals/group) were processed under binary, selecting find maxima. Noise tolerance was set uniformly at 10 and output set to identify single pixels whilst excluding edge maxima. Data is presented as luciferase expression/×40 field of view.

3.13. Statistical analysis

Results presented are representative data from a minimum of three separate experiments with at least three experimental replicates per group, unless otherwise stated. High throughput screening of the entire Pharmacological Diversity Drug-like Set compound library was performed once but all hits were subjected to subsequent analysis as indicated. Where necessary, data were normalised by logarithmic transformation. Data are represented as mean ± standard error of the mean (SEM). Statistical significance was calculated using 2-sample, 2-tailed student's t-tests or one way ANOVA followed by Dunnett's post-hoc test. $p < 0.05$ was considered statistically significant.

4. Results

4.1. HTS for inhibitors of FX-mediated Ad5 transduction

It has been previously described that co-incubation of Ad5 with physiological levels of FX (10 μg/ml) causes a substantial increase in Ad5 transduction *in vitro* and *in vivo* compared to Ad5 alone [13,16]. In this study, initial optimisation and validation experiments were performed to convert this frequently employed *in vitro* assay into a high throughput cell-based screen in order to test a diverse library of compounds for their ability to inhibit FX-mediated Ad5 transduction. The assay was adapted to a 384-well format employing SKOV3 cells, a cell line susceptible to FX-mediated Ad infection [16], and an Ad5 vector expressing a GFP transgene. 10,240 low molecular weight compounds from the Pharmacological Diversity Drug-like Set were screened at a concentration of 10 μM in the presence of 10 μg/ml FX in triplicate. At 48 h post-infection cells were fixed and stained with Hoechst 33342 and propidium iodide, then imaged and analysed using the In Cell Analyzer 2000 and Developer Toolbox V1.6 software (Fig. 1A and B). Ad5GFP expression was treated as the primary readout, with clear MIN (minus FX) and MAX (plus FX) controls on each plate, providing a broad signal window in which to identify compounds that blocked Ad5 transduction in the presence of FX (Fig. 1A, C and D). In order to prevent skewing of results due to compound toxicity non-viable cells were discarded from the analysis (Fig. 1B) and a measure of GFP intensity per viable cell per field of view was calculated. The 1% DMSO vehicle
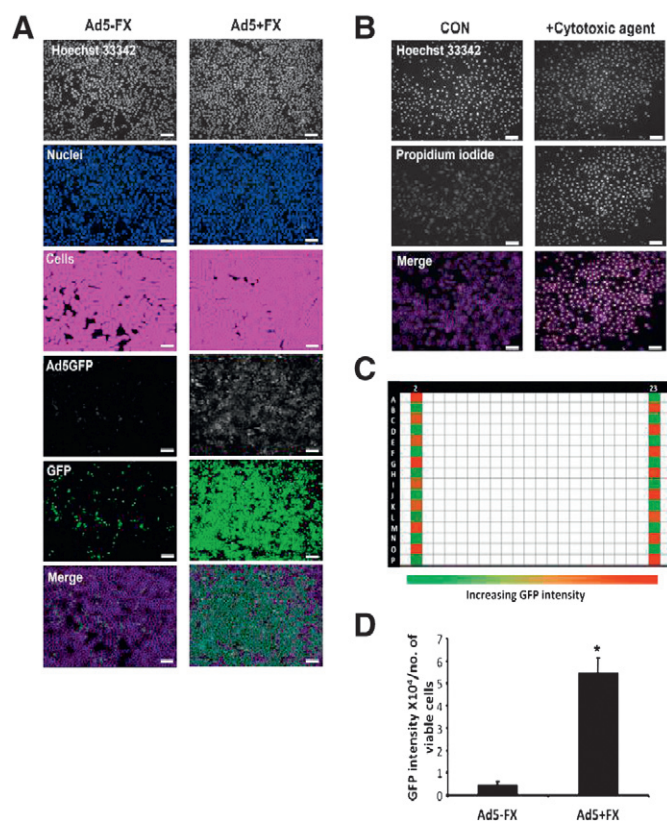

Fig. 1. The HTS methodology. (A) SKOV3 cells were incubated with 1000 vp/cell of Ad5GFP in the absence or presence of FX. 48 h post-infection cells were fixed and stained with Hoechst 33342, imaged using the IN Cell Analyzer 2000 and analysed using the IN Cell Developer Toolbox. Nuclei, cells and GFP expression were segmented based on their staining, size, shape and intensity. The outline of each of these parameters was highlighted using the software bitmap overlay; the nuclei are shown in blue, the cells in pink and the GFP in green. (B) Cells were infected with 1000 vp/cell of Ad5 in the absence or presence of 40 μM T0501-7827 (Enamine, Ukraine), a cytotoxic compound. After 48 h cells were fixed and stained with Hoechst 33342 and propidium iodide, imaged and analysed. Non-viable cells were segmented based on propidium iodide staining. Once parameters were defined, the IN Cell Developer Toolbox was used to calculate the number of viable cells. 10× magnification, scale bars = 50 μm. (C) Trellis heat map of the assay plate highlighting the plus (red) and minus (green) FX control conditions. (D) SKOV3 cells were incubated with 1000 vp/cell of Ad5GFP in the absence or presence of FX and GFP transgene expression was quantified at 48 h using the IN Cell Developer Toolbox. GFP expression was normalised to the number of viable cells. *$p < 0.05$ as compared to Ad5 − FX control.

caused no effect on assay performance (Supplementary Fig. 1A and B). Test data were normalised to plus and minus FX control conditions and data represented as percentage inhibition of FX-mediated Ad5GFP expression. The suitability of this assay for a HTS was verified in initial experiments, having a signal to background ratio of 29.82 ± 3.93-fold and an average Z′ factor > 0.5 [22]. A plot of the percent inhibition from the 32 sets of assay plates classified by plate row and the plate row median data value indicated that the assay was well behaved and the majority of compounds were inactive and exhibited activity levels similar to the plus FX control conditions (*i.e.* ≤0% inhibition of FX-mediated Ad5 gene transfer) (Fig. 2A and B). Hits were identified as those causing >75% inhibition of FX-mediated Ad5 transduction. From the primary screen and secondary rounds of screening 17 compounds (0.16% of initial library) were identified (Fig. 2C and D). Upon exclusion of compounds causing toxicity, non-reproducible effects or those with structural features which may exhibit bias towards compound promiscuity, three hit compounds (0.029% hit rate) were selected for detailed analysis.
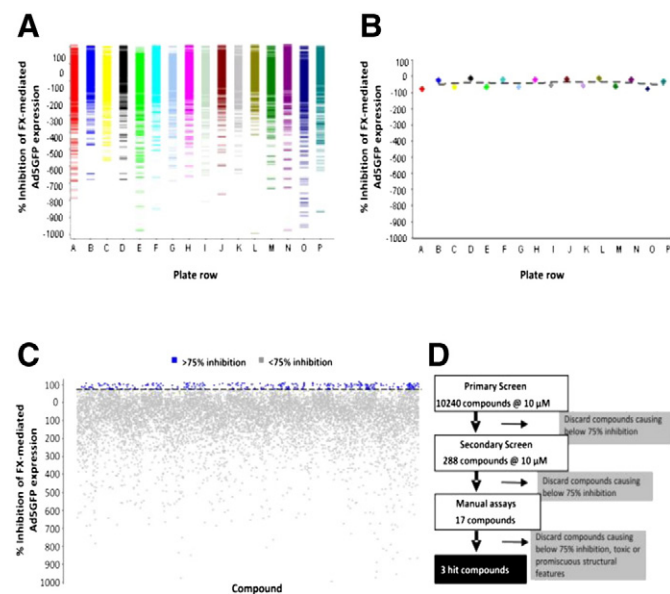
Fig. 2. Candidate screen hits. Cells were incubated with 1000 vp/cell of Ad5GFP in the absence or presence of FX plus 10 μM compound (Pharmacological Diversity Drug-like set − 10,240 in total). At 48 h the cells were fixed and stained, then screened for their ability to inhibit FX-mediated Ad5GFP expression. Data was normalised to minus and plus FX control conditions and represented as percentage inhibition. (A) Graphical summary of the HTS data categorised by plate rows A to P. Each row is separated by colour. (B) Plot of plate row median percentage inhibition of FX-mediated Ad5GFP expression showing the median trendline. (C) Each dot represents an individual compound. Compounds causing >75% inhibition, as shown above the dashed line, are highlighted in blue. (D) Schematic review of the HTS process.

4.2. Validation and structural analysis of hit compounds T5660138, T5424837 and T5550585

The three hit compounds identified were T5660138 (abbreviated to T138), T5424837 (T837) and T5550585 (T585). All three compounds ablated FX-mediated Ad5 transduction, in the absence of cytotoxicity (Fig. 3A and B). Compounds T138, T837 and T585 possess several common structural features (Fig. 3C and D). Compounds T585 and T138 share a similar 3-phenyl-5-methlene-1,2,4-oxadiazole moiety, whereas T138 and T837 have similar substituted condensed heterocyclic systems bridged to a 5-membered heterocyclic ring *via* two atom linkers (Fig. 3C and D). Hence, compound T138 has features that overlap with both T585 and T837. In order to align all three molecules simultaneously, a pharmacophore hypothesis was formed (Fig. 3D). The minimal core can be defined as two heterocyclic moieties bridged *via* a 1–2 atom linker. The first moiety is a 5-membered electron rich heterocycle which may serve as a H-bond acceptor as well as a participant in van der Waals contacts. The second moiety, larger by volume, is a lipophilic, condensed heterocycle system that may serve as a bulk van der Waals contributor and the quinazoline and 1,3-benzodiaxane of T138 and T837, respectively, along with the 4-nitro-3,5-dimethyl-1,2-pyrazole of T585 are putative representatives. Therefore the pharmacophore model was defined as 5-membered heterocycle with hydrogen bond acceptor and aromatic features linked to a bulky lipophilic feature.

4.3. Activity of T138, T837 and T585 and compound analogues

Based on the established pharmacophore model, for every primary hit a follow-up library was designed. Compounds that resemble the minimalistic core with various substitutions on the periphery were identified in stock collections. An additional 28 compounds were selected and preliminary structure activity relationship analysis was performed using this follow-up library. Several modifications to the parental scaffold decreased the ability to block FX-mediated Ad5
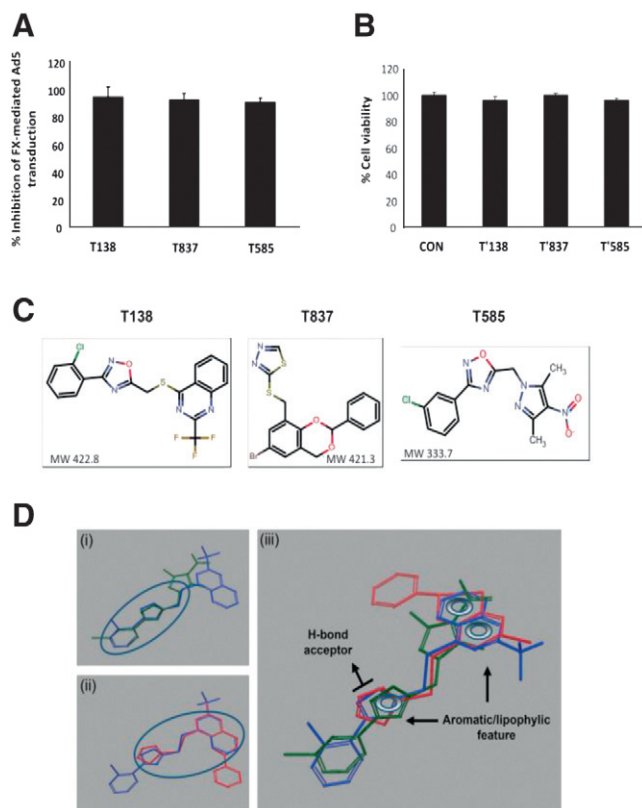

Fig. 3. Identification of the primary hit compounds. (A) Cells were infected with 1000 vp/cell of Ad5 in the absence or presence of FX and 10 μM compounds T138, T837 and T585. Transgene expression was measured 45 h post-infection. Results were adjusted to ±FX controls. (B) Cell viability was assessed after 48 h co-incubation with each compound. Error bars represent SEM (n = 4/compound). (C) Chemical structures of T138, T837 and T585. (D) (i) T585 (green) with T138 (blue) and (ii) T138 (blue) with T837 (red). Zones of high topological identity are highlighted. (iii) Structural alignment of all three hits. Common minimal pharmacophore core is shown: 5-membered heterocycle with hydrogen bond acceptor and aromatic feature linked to a bulky lipophilic feature.

transduction (Supplementary Figs. 2, 3 and 4). Screening results of the follow-up library also revealed novel hits with similar or improved activity. In an attempt to rank the analogue compounds based on inhibition and potency, the IC_{50} of the three parent compounds T138, T837 and T585 and the most active analogues were determined. All compounds had IC_{50} values below 5.5 μM (Fig. 4). Data revealed compound T136, a *meta*-chlorine substituted analogue of the parent, had the most potent effect on FX-mediated Ad5 transduction, having a 4-fold improved IC_{50} of 1 μM compared to 4.01 μM for T138 (Fig. 4A). Similarly with regard the T585 compound family the substitution of the chlorine from a *meta* to a *para* position was well tolerated, as shown by the enhanced activity of compound T402 (Fig. 4B). Finally, compound T956 caused the greatest level of inhibition at the highest concentration of 10 μM, despite having an extra benzyl ring to its parent compound T837 (Fig. 4C). These findings validate the suggested pharmacophore model and initial hit compounds.

4.4. Active compounds do not interfere with Ad5:FX complex engagement but disrupt a later step of the transduction pathway

A recent study by Xu et al. has shown that FX coating the Ad5 hexon can in fact shield the virus from attack from the classical complement system, thereby protecting the virus from neutralisation in the blood [6]. Therefore it was important to investigate whether the compounds were interfering with direct Ad5:FX complex engagement. To examine if the compounds hindered Ad5 binding to FX, SPR analysis was performed. 10 μM compound or an equivalent volume of DMSO was
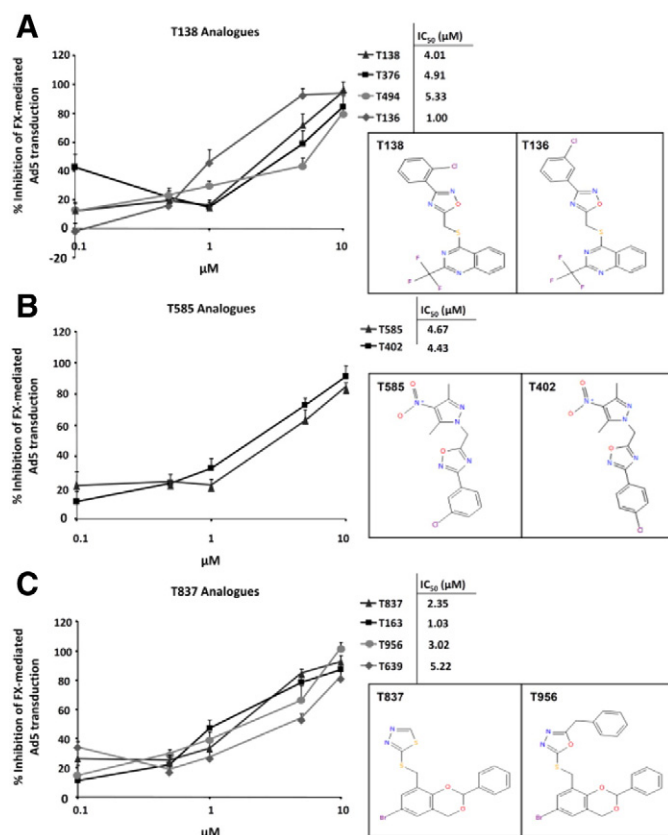
Fig. 4. IC_{50} evaluation of hits and compound analogues. Cells were infected with Ad5 in the absence or presence of FX plus 0.1, 0.5, 1, 5 or 10 μM (A) T138, (B) T585 or (C) T837 and chemically related compounds. Transgene expression was measured after 48 h. Data was normalised to minus and plus FX control conditions and represented as percentage inhibition. Error bars represent SEM (n = 4/compound). The IC_{50} values for each of the compounds were calculated by fitting a 4-parameter logistic non-linear regression model equation using MasterPlex ReaderFit analysis software.

Fig. 5. Compounds act post Ad5:FX engagement (A) Sensorgrams of Ad5 in the presence of 10 μM compound or an equivalent volume of DMSO injected over FX for ~200 s at a flow rate of 30 μl/min. Sensorgrams are subtracted for blank injections. (B) A549 cells were infected with Ad5 ± FX and μM compound and transgene expression was measured at 48 h. (C) A549 cells were incubated with 10,000 vp/cell of Alexa488-labelled Ad5 ± FX and 10 μM compound for 1 h at 4 °C, followed by incubation at 37 °C for 180 min prior to staining for the MTOC marker pericentrin. Complete colocalisation of Ad5 with pericentrin was calculated by analysing at least 5 separate 40× microscope fields per experimental condition. *$p < 0.05$ as compared to −FX conditions or #$p < 0.05$ as compared to −FX.

preincubated with Ad5 and then injected over FX immobilised on the chip (Fig. 5A). When the Ad5 and DMSO control was passed over FX, there was an increase in response units (up to ~60 RU), indicating Ad5 binding to FX. When Ad5 in the presence of each of the compounds was passed over the chip, there was a similar increase in response units. This suggests that the incubation of Ad5 with the transduction inhibitors does not interfere with Ad5 binding directly to FX. Next, we examined whether the compounds could block Ad5 transduction *via* different established routes of Ad5 cell engagement and subsequent entry. The CAR pathway was therefore assessed, in addition to FX-mediated transduction. A549 cells were used as they express significant levels of CAR and are also susceptible to FX-mediated Ad5 infection [16]. Under control conditions, Ad5 transduction was significantly increased in the presence of FX (~6-fold) (Fig. 5B). All compounds ablated Ad5 transduction in the absence and presence of FX (Fig. 5B). This data demonstrated the capability of the six compounds to inhibit both CAR and FX-mediated Ad5 transduction *in vitro*. Subsequently, effects of the compounds on Ad5 intracellular transport were investigated. Alexa-488 fluorescently labelled Ad5 transport to the MTOC was assessed in the absence and presence of 10 μM compound. Intracellular trafficking was disrupted by each of the inhibitors (Fig. 5C). Instead of forming a punctate localisation at the MTOC [16], virus localisation was diffuse in the perinuclear region in the presence of each of the compounds. When the percentage of cells with which the virus particles colocalised with the MTOC was quantified, colocalisation was significantly reduced with all inhibitors (Fig. 5C). These data indicate that in the presence of the compounds post-entry intracellular trafficking of Ad5 to the nucleus was disrupted.
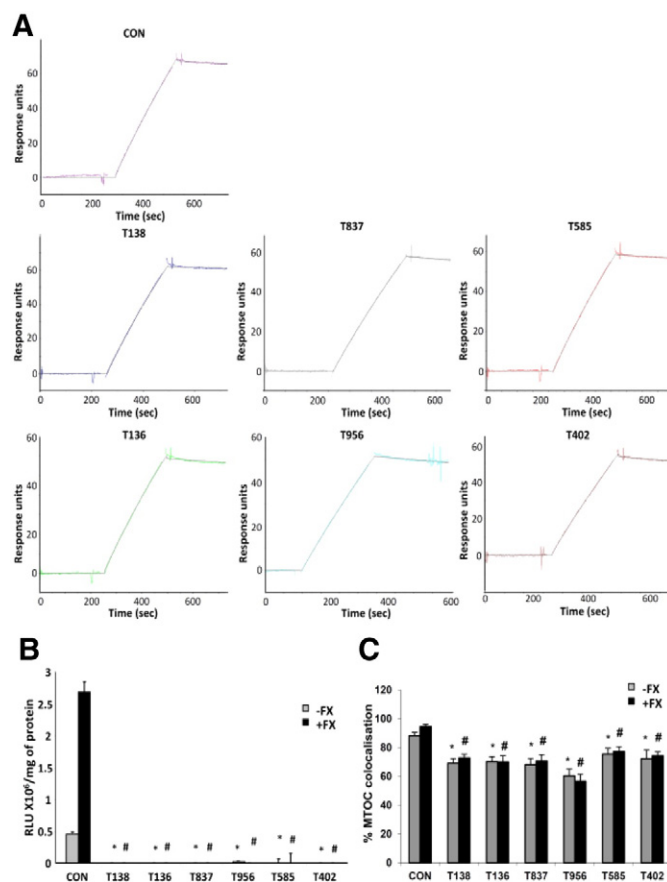
4.5. T138 and its analogue T136 decrease Ad5 transduction in vivo without the elevation of toxicity markers

As T138 and T136 possess structural features common to both the other two families (T837 and T585) these compounds were tested *in vivo* to investigate whether the compounds decreased Ad5 liver transduction. Prior to *in vivo* testing, we investigated if the compounds were interfering with the stability of the viral particles. Circular dichroism (CD), a method for examining the extent and rate of structural changes of a protein [23], was used to assess the effect of incubation of 10 μM compound with the virus (Supplementary Fig. 5). CD spectra analysis indicated that for Ad5 + T138 the mid-point of protein unfolding occurred at ~45 °C as opposed to ~47 °C in the case of Ad5 + DMSO control and Ad5 + T136 conditions (Supplementary Fig. 5). As this modest effect of T138 on virus stability occurred above temperatures relevant to our assays (37 °C), and T136 had no effect on thermostability of Ad5, it was concluded that the compounds were not affecting the stability of the virus used in this study. For *in vivo* experimentation, MF1 mice were injected intravenously with a high dose of 1×10^{11} vp/mouse of Ad5 luciferase or Ad5 which has been preincubated with 10 μM T138, 10 μM T136 or an equivalent volume of the vehicle. Luciferase transgene expression was visualised by whole-body bioluminescence imaging and

quantified 48 h after administration. As expected, Ad5 targeted the liver as evidenced by the high levels of luciferase expression visually and quantitatively assessed by bioluminescence imaging at 48 h post-injection (Fig. 5A and B). There was no significant difference observed in the Ad5 plus DMSO control group, indicating that the vehicle did not cause an effect on Ad5 transduction *in vivo* (Fig. 5A and B). However, in the presence of T138 and T136 there were 6.7-fold and 4.6-fold decreases respectively in luciferase expression compared to Ad5 and Ad5 plus DMSO control conditions (Fig. 5A and B). In addition, immunohistochemistry was performed for luciferase transgene expression in frozen liver and spleen sections (Fig. 6C, D and Supplementary Fig. 5). In concordance with the bioluminescent imaging data, a significant reduction in luciferase transgene expression in the livers of animals treated with Ad5 in the presence of T136 and T138 was observed. This indicates that these two closely related compounds exhibit activity *in vivo*, decreasing hepatic transduction of Ad5. There was no significant difference between the groups in the levels of luciferase transgene expression in spleen sections as shown by immunofluorescence analysis (Fig. 6D and Supplementary Fig. 6). The elevation of serum transaminases, such as AST and ALT levels can be an indicator of acute toxicity *in vivo*. Therefore we analysed serum samples taken from mice 48 h post-injection of virus ± compound for the levels of AST and ALT to see if the compounds were having a toxic side effect. We found no significant difference in either serum transaminase between the Ad5 control, Ad5+DMSO, Ad5+T138 or Ad5+T136 groups of animals.

Fig. 6. Effect of hit compounds on Ad5 transduction *in vivo*. (A) Luciferase expression visualised by whole-body bioluminescence imaging 48 h after intravascular administration of 1×10^{11} vp/mouse Ad5 alone, Ad5 in the presence of 10 μM T138, 10 μM T136 or DMSO in 200 μl PBS or PBS alone in MF1 mice. (B) Luciferase expression as assessed by whole-body bioluminescence imaging was quantified at 48 h. (C) Luciferase expression in frozen liver sections (5 μm) was detected by immunofluorescence. Scale bar = 50 μm. (D) Luciferase expression in frozen liver and spleen sections were quantified using Image J software by analysing at least 10 separate images from 40× microscope fields per experimental condition. *p < 0.05 as compared to Ad5 control conditions. (E and F) Serum transaminases, (E) aspartate aminotransferase (AST) and (F) alanine aminotransferase (ALT) were quantified 48 h postinjection of 1×10^{11} vp/mouse.

5. Discussion

Adenoviruses continue to hold great promise for a vast number of gene, viral and vaccination applications. However, virus binding to host factors results in liver sequestration and potent innate immune and inflammatory responses. This compromises vector efficacy and is of clear concern for the successful use of Ads in the clinical setting. This study focused on developing a small molecule inhibitor approach to block Ad transduction mediated by FX, a key host determinant of the hepatic tropism and viral immune recognition [13,18].

Improvements in the understanding of Ad infection pathways *in vitro* and key *in vivo* tropism determining interactions have allowed the design of assays with more realistic and relevant parameters for the identification of new drugs [13,23]. Recently it was found that species D Ad37 infection causes epidemic keratoconjunctivitis by binding of the Ad fibre knob protein to glycoproteins containing two terminal sialic acid moieties on the surface of epithelial cells in the cornea or conjunctiva [24]. This finding led to Spjut et al. synthesizing tri- and tetra-valent sialic acid compounds which effectively block Ad37 infection of human ocular cells. SPR and crystallography techniques demonstrated that the trivalent sialic acid conjugate, ME0322, binds directly to the sialic acid-binding sites in the fibre knob, with similar affinity to GD1a hexasaccharide, and is a potent inhibitor of Ad37 infection [25]. A separate study reported the use of multivalent sialic acid constructs and the development of "molecular wipes" for the topical treatment of Ad induced epidemic keratoconjunctivitis [26]. These studies highlight the current advancements in pharmacological inhibitory agents for use against Ads from species D, progress which is largely due to the increasing knowledge of Ad cell/organ interaction mechanisms.

Studies have shown that once the virus comes into contact with the bloodstream FX is the major mediator of Ad liver transduction [13,14]. An array of simple and diverse assays exists to study Ads and manipulate their interactions *in vitro*. In this study the FX-mediated Ad5 transduction pathway and routinely used cell-based protocols were exploited to design a unique and robust Ad5 fluorescence reporter gene- and cell-based HTS. It was hypothesised that identification of an inhibitor of Ad transduction in the presence of FX using a relevant *in vitro* set-up within a time frame sufficient to allow the key steps of infection to occur (48 h), could have potential in an *in vivo* setting. The assay developed in this study is highly adaptable. For example a fluorescently-labelled virus could be employed to investigate inhibitors or enhancers of cellular binding or stages of the post-entry infection process. As the assay has an easily measured readout it is a useful and rigorous approach for the discovery of novel compounds that interfere with Ad infection processes. For instance, a number of the compounds screened in this assay caused a substantial enhancement of FX-mediated Ad5GFP expression, with compounds enhancing Ad5 gene transfer by up to 10-fold (Fig. 2C). In the cancer gene/viral therapy setting, compounds which increase the Ad5 transduction capability immediately after localised injection may be an attractive option for improved treatment of solid tumours. This type of strategy could also be adapted for the treatment of cardiovascular diseases, *via* coating stents with the Ad:FX:compound complex to improve direct virus uptake in the vessel wall. Investigation of potential Ad transduction enhancers identified from this screen certainly warrants further study.

Previously the generation of compounds in screening libraries was directed by chemical structures and selectivities rather than on pharmacological properties. In this regard, *in vitro* affinities were optimised at the potential expense of solubility, metabolic stability and permeability properties and often compounds which appear to be promising lead candidates are not always suitable for further medicinal chemistry exploration which precludes their progression [27]. Screening libraries of compounds with drug-like properties is now seen as preferable, possessing improved ADME and toxicity profiles. Design of the Pharmacological Diversity Drug-like Set was based on pharmacological features rather than on the chemical structure of
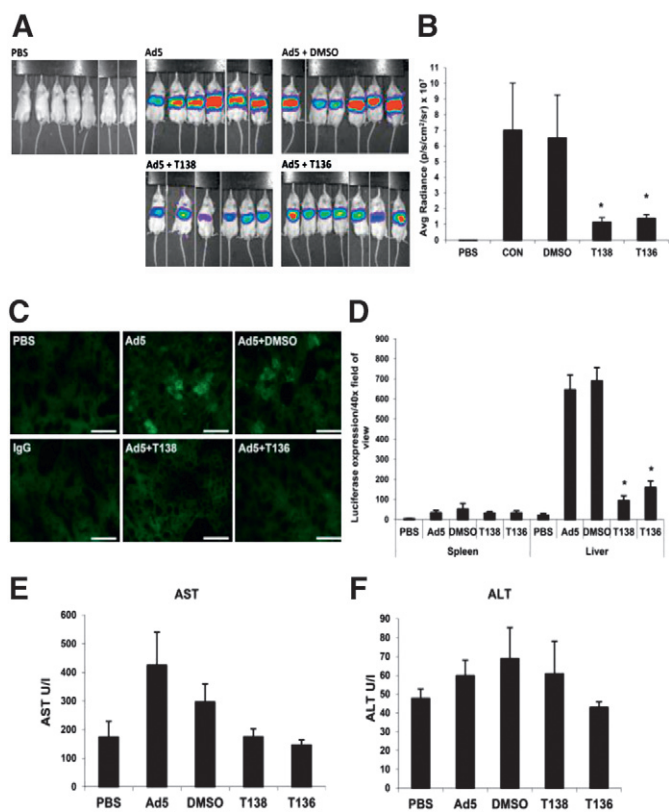
compounds. From multiple rounds of screening the three repeat positive hits identified (T138, T585, T837 (0.029% confirmed hit rate)) as efficiently ablating FX-mediated Ad transduction were found to possess common structural features, fitting into the one pharmacophore model. Moreover, the fact that T138 had similar features to both T585 and T837 adds confidence to the reliability of the experiment and screening validity. Importantly the effects of these compounds occurred in the absence of any cytotoxicity, and the lack of toxic signatures can be an important factor for downstream medicinal chemistry. This initial pharmacophore model was further validated by the screening of analogues and the identification of the new hits T136, T402 and T956, with low micromolar potency. The enhanced IC_{50} values for several of the analogues compared to the parent compound provide a proof of principle that the characteristics of these compounds can be improved and thus help to certify the structures as a starting point for the development of such a small molecule inhibitor.

The recent work by Xu et al., showing the ability of FX to protect the virus from attack by natural antibodies and complement, may alter the way we design liver detargeting strategies for intravascular gene therapy applications [6]. The compounds identified here, do not hinder the Ad5:FX interaction but are effective at blocking a later step of the transduction pathway. This may be advantageous in that the virus would still acquire the protective FX coat thus evading activation of immune pathways whilst still avoiding transgene expression mediated *via* this pathway. Alternatively the high throughput screen could have been designed differently to look more specifically at blocking only FX-mediated Ad transduction *i.e.* search for inhibitors of Ad5:FX complex binding to the cell surface. There are several ways such an assay could be designed, such as employing SPR to screen compounds for those which blocked Ad5:FX binding, or if a cell-based assay was preferable measuring the effect of compounds on fluorescently-labelled Ad5 binding in SKOV3 cells. Potent compound effects *in vitro* do not necessarily translate in the *in vivo* setting [28]. However in this instance, *in vivo* T138 and its closely related analogue T136 significantly reduced transgene expression at 48 h post-intravenous administration of a high viral dose (1×10^{11} vp/mouse). This dose of virus was chosen as it was previously demonstrated to cause high levels of liver transduction in mice [19], thereby providing a clear measure of compound effect. The activity shown by T138 and T136 *in vivo* was a very promising result and this biological effect signifies the translational potential of the compounds.

It would be of significant interest to study the effect of these inhibitors on the hepatic uptake of different FX-binding serotypes and to investigate their influence on the retargeting capability of the vector. It may be that the compounds successfully decrease Ad liver transduction but allow for transgene expression of a modified vector in target cells/tissues mediated *via* an alternate receptor *e.g.* integrin-mediated transduction. Biodistribution studies could be performed by coincubation of compound with an integrin targeted vector such as Ad5RGD4C, which has been genetically engineered to contain a αv integrin binding ligand in the HI loop [29,30], to assess effects on vector transduction. Furthermore, it would be of worth to investigate if blocking the FX pathway using this small molecule inhibitor approach would alter the FX associated innate and inflammatory immune response. Comparing the early immune response post-administration of Ad5 in the presence of T136 and T138 with that following delivery of an Ad5 FX-binding ablated vector alone could have value. In addition, the compounds identified in this study may also function as an anti-viral agent in the case of disseminated adenovirus infections. Ads have emerged as a significant pathogen associated with high morbidity and mortality in immunocompromised individuals (*e.g.* sufferers of hereditary immune deficiencies, AIDS patients, haematopoietic stem cell transplant recipients undergoing immunosuppressive treatment). Whilst in healthy individuals Ad infection is mostly self-limiting, in the immunocompromised host Ads exploit the impaired immunological response and can become invasive causing prolonged, severe and even life threatening disease. There are however,

currently no formally approved selective antiviral agents available that treat Ad infection thus these compounds may have potential in the development of a novel anti-adenoviral agent.

To conclude, we propose the optimisation and development of the compounds identified in this study, in particular T138 and T136, which cause a potent effect *in vitro* and a substantial reduction in Ad5 gene transfer *in vivo*, as a novel strategy to prevent FX-mediated Ad5 transduction for gene therapy applications.

Appendix A. Supplementary data

Supplementary data to this article can be found online at http://dx.doi.org/10.1016/j.jconrel.2013.05.007.

References

[1] M.L. Edelstein, M.R. Abedi, J. Wixon, Gene therapy clinical trials worldwide to 2007—an update, J. Gene Med. 9 (2007) 833–842.

[2] M.R. Duffy, A.L. Parker, A.C. Bradshaw, A.H. Baker, Manipulation of adenovirus interactions with host factors for gene therapy applications, Nanomedicine 7 (2012) 271–288.

[3] N.C. Di Paolo, E.A. Miao, Y. Iwakura, K. Murali-Krishna, A. Aderem, R.A. Flavell, T. Papayannopoulou, D.M. Shayakhmetov, Virus binding to a plasma membrane receptor triggers interleukin-1 ± -mediated proinflammatory macrophage response in vivo, Immunity 31 (2009) 110–121.

[4] J. Huard, H. Lochmuller, G. Acsadi, A. Jani, B. Massie, G. Karpati, The route of administration is a major determinant of the transduction efficiency of rat tissues by adenoviral recombinants, Gene Ther. 2 (1995) 107–115.

[5] A. Lieber, C. He, L. Meuse, D. Schowalter, I. Kirillova, B. Winther, M. Kay, The role of Kupffer cell activation and viral gene expression in early liver toxicity after infusion of recombinant adenovirus vectors, J. Virol. 71 (1997) 8798–8807.

[6] Z. Xu, Q. Qiu, J. Tian, J.S. Smith, G.M. Conenello, T. Morita, A.P. Byrnes, Coagulation factor X shields adenovirus type 5 from attack by natural antibodies and complement, Nat. Med. (2013), http://dx.doi.org/10.1038/nm.3107.

[7] M. Lyons, D. Onion, N.K. Green, K. Aslan, R. Rajaratnam, M. Bazan-Peregrino, S. Phipps, S. Hale, V. Mautner, L.W. Seymour, K.D. Fisher, Adenovirus type 5 interactions with human blood cells may compromise systemic delivery, Mol. Ther. 14 (2006) 118–128.

[8] R.C. Carlisle, Y. Di, A.M. Cerny, A.F.-P. Sonnen, R.B. Sim, N.K. Green, V. Subr, K. Ulbrich, R.J.C. Gilbert, K.D. Fisher, R.W. Finberg, L.W. Seymour, Human erythrocytes bind and inactivate type 5 adenovirus by presenting Coxsackie virus-adenovirus receptor and complement receptor 1, Blood 113 (2009) 1909–1918.

[9] M. Othman, A. Labelle, I. Mazzetti, H.S. Elbatarny, D. Lillicrap, Adenovirus-induced thrombocytopenia: the role of von Willebrand factor and P-selectin in mediating accelerated platelet clearance, Blood 109 (2007) 2832–2839.

[10] D. Stone, Y. Liu, D. Shayakhmetov, Z.-Y. Li, S. Ni, A. Lieber, Adenovirus–platelet interaction in blood causes virus sequestration to the reticuloendothelial system of the liver, J. Virol. 81 (2007) 4866–4871.

[11] H. Jiang, Z. Wang, D. Serra, M.M. Frank, A. Amalfitano, Recombinant adenovirus vectors activate the alternative complement pathway, leading to the binding of human complement protein c3 independent of anti-Ad antibodies, Mol. Ther. 10 (2004) 1140–1142.

[12] A.L. Parker, S.N. Waddington, C.G. Nicol, D.M. Shayakhmetov, S.M. Buckley, L. Denby, G. Kemball-Cook, S. Ni, A. Lieber, J.H. McVey, S.A. Nicklin, A.H. Baker, Multiple vitamin K-dependent coagulation zymogens promote adenovirus-mediated gene delivery to hepatocytes, Blood 108 (2006) 2554–2561.

[13] S.N. Waddington, J.H. McVey, D. Bhella, A.L. Parker, K. Barker, H. Atoda, R. Pink, S.M.K. Buckley, J.A. Greig, L. Denby, J. Custers, T. Morita, I.M.B. Franciscetti, R.Q. Monteiro, D.H. Barouch, N. van Rooijen, C. Napoli, M.J.E. Havenga, S.A. Nicklin, A.H. Baker, Adenovirus serotype 5 hexon mediates liver gene transfer, Cell 132 (2008) 397–409.

[14] O. Kalyuzhniy, N.C. Di Paolo, M. Silvestry, S.E. Hofherr, M.A. Barry, P.L. Stewart, D.M. Shayakhmetov, Adenovirus serotype 5 hexon is critical for virus infection of hepatocytes in vivo, Proc. Natl. Acad. Sci. 105 (2008) 5483–5488.

[15] M.R. Duffy, A.C. Bradshaw, A.L. Parker, J.H. McVey, A.H. Baker, A cluster of basic amino acids in the factor X serine protease mediates surface attachment of adenovirus/FX complexes, J. Virol. 85 (2011) 10914–10919.

[16] A.C. Bradshaw, A.L. Parker, M.R. Duffy, L. Coughlan, N. van Rooijen, V.-M. Kähäri, S.A. Nicklin, A.H. Baker, Requirements for receptor engagement during infection by adenovirus complexed with blood coagulation factor X, PLoS Pathog. 6 (2010) e1001142.

[17] R. Alba, A.C. Bradshaw, A.L. Parker, D. Bhella, S.N. Waddington, S.A. Nicklin, N. van Rooijen, J. Custers, J. Goudsmit, D.H. Barouch, J.H. McVey, A.H. Baker, Identification of coagulation factor (F)X binding sites on the adenovirus serotype 5 hexon: effect of mutagenesis on FX interactions and gene transfer, Blood 114 (2009) 965–971.

[18] K. Doronin, J.W. Flatt, N.C. Di Paolo, R. Khare, O. Kalyuzhniy, M. Acchione, J.P. Sumida, U. Ohto, T. Shimizu, S. Akashi-Takamura, K. Miyake, J.W. MacDonald, T.K. Bammler, R.P. Beyer, F.M. Farin, P.L. Stewart, D.M. Shayakhmetov, Coagulation factor X activates innate immunity to human species C adenovirus, Science 338 (2012) 795–798.

[19] R. Alba, A.C. Bradshaw, L. Coughlan, L. Denby, R.A. McDonald, S.N. Waddington, S.M.K. Buckley, J.A. Greig, A.L. Parker, A.M. Miller, H. Wang, A. Lieber, N. van Rooijen, J.H. McVey, S.A. Nicklin, A.H. Baker, Biodistribution and retargeting of FX-binding ablated adenovirus serotype 5 vectors, Blood 116 (2010) 2656–2664.

[20] D.J. Von Seggern, J. Kehler, R.I. Endo, G.R. Nemerow, Complementation of a fibre mutant adenovirus by packaging cell lines stably expressing the adenovirus type 5 fibre protein, J. Gen. Virol. 79 (1998) 1461–1468.

[21] A. Lagunin, A. Stepanchikova, D. Filimonov, V. Poroikov, PASS: prediction of activity spectra for biologically active substances, Bioinformatics 16 (2000) 747–748.

[22] J.-H. Zhang, T.D.Y. Chung, K.R. Oldenburg, A simple statistical parameter for use in evaluation and validation of high throughput screening assays, J. Biomol. Screen. 4 (1999) 67–73.

[23] R.D. Gillard, Circular dichroism. A review, Analyst 88 (1963) 825–828.

[24] E.C. Nilsson, R.J. Storm, J. Bauer, S.M.C. Johansson, A. Lookene, J. Angstrom, M. Hedenstrom, T.L. Eriksson, L. Frangsmyr, S. Rinaldi, H.J. Willison, F.P. Domellof, T. Stehle, N. Arnberg, The GD1a glycan is a cellular receptor for adenoviruses causing epidemic keratoconjunctivitis, Nat. Med. 17 (2011) 105–109.

[25] S. Spjut, W. Qian, J. Bauer, R. Storm, L. Frängsmyr, T. Stehle, N. Arnberg, M. Elofsson, A potent trivalent sialic acid inhibitor of adenovirus type 37 infection of human corneal cells, Angew. Chem. Int. Ed. 50 (2011) 6519–6521.

[26] K. Aplander, M. Marttila, S. Manner, N. Arnberg, O. Sterner, U. Ellervik, Molecular wipes: application to epidemic keratoconjuctivitis, J. Med. Chem. 54 (2011) 6670–6675.

[27] K.H. Bleicher, H.-J. Bohm, K. Muller, A.I. Alanine, Hit and lead generation: beyond high-throughput screening, Nat. Rev. Drug Discov. 2 (2003) 369–378.

[28] M.B. Ortigoza, O. Dibben, J. Maamary, L. Martinez-Gil, V.H. Leyva-Grado, P. Abreu Jr., J. Ayllon, P. Palese, M.L. Shaw, A novel small molecule inhibitor of influenza A viruses that targets polymerase function and indirectly induces interferon, PLoS Pathog. 8 (2012) e1002668.

[29] I. Dmitriev, V. Krasnykh, C.R. Miller, M. Wang, E. Kashentseva, G. Mikheeva, N. Belousova, D.T. Curiel, An adenovirus vector with genetically modified fibers demonstrates expanded tropism via utilization of a coxsackievirus and adenovirus receptor-independent cell entry mechanism, J. Virol. 72 (1998) 9706–9713.

[30] D. Majhen, J. Nemet, J. Richardson, J. Gabrilovac, M. Hajsig, M. Osmak, M. Eloit, A. Ambriović-Ristov, Differential role of $\alpha v \beta 3$ and $\alpha v \beta 5$ integrins in internalization and transduction efficacies of wild type and RGD4C fiber-modified adenoviruses, Virus Res. 139 (2009) 64–73.